Instantaneous Shape and Segmental Density of Individual Flexible Linear Macromolecules. 4. Tagged in Untagged Crystallizable Polymers

S. M. Aharoni,* V. Kramer, and D. A. Vernick

Corporate Research Center, Allied Chemical Corporation, Morristown, New Jersey 07960.
Received August 24, 1978

ABSTRACT: Monomolecular dispersions of iodine-tagged high molecular weight isotactic polystyrene (TiPS) in untagged isotactic polystyrene (iPS) were prepared. By means of transmission electron microscopy through the microtomed bulk, and microdensitometry across imaged molecules, it was found that the amorphous TiPS molecules are neither spherical nor have a smooth bell-shaped segmental distribution. The shape is irregular and the segmental density reveals 100 to 250 Å size submolecular domains of high segmental density intermixed with regions of lower density. In solution cast films and in annealed molded films, nascent crystallization of the TiPS was observed. Small crystallites and minute lamellae are initially formed within the confines of the parent molecules. The indication is that incipient crystallization occurs within the molecule and involves one or more of the higher density submolecular domains. Then, co-crystallization with domains belonging to other macromolecules takes place. Such crystallization requires no large scale intermolecular disentanglements or long-range molecular transport. It also leaves the radius of gyration of the molecule unchanged upon going from the melt to the semicrystalline solid. Observations on bromine-tagged ultra-high molecular weight polyethylene in untagged polyethylene lead to similar conclusions.

In the four previous papers of this series we have demonstrated that, in the absence of phase separation, individual macromolecules of tagged poly-*cis*-isoprene (PIP) in untagged PIP,[1,2] tagged PIP in a polyisobutylene (PIB) matrix,[3] and tagged polystyrene (PS) in untagged PS[4] possess neither spherical symmetry nor a smooth Gaussian segmental distribution. In these three cases the instantaneous shape of tagged individual molecules was irregular. Internally, the segmental distribution appears as an association of high-density regions intermixed with regions of lower density. The high-density regions tend, on the average, to be closer to the geometrical center of the macromolecule. From microdensitometer scans across the images of the macromolecules on the electron image plates, the size of the high-density submolecular domains is estimated to be 300 to 400 Å for the PIP and 100 to 200 Å for the PS.[4]

Upon averaging a large number of densitometer scans across individual macromolecules of about the same size, one obtains a smooth bell-shaped segmental distribution,[3] in agreement with such observations as small-angle neutron scattering (SANS) or small-angle X-ray scattering (SAXS), where the results are averaged over a large population of macromolecules, and over all angles.

In the studies above, high molecular weight molecules were tagged and observed in the bulk. Their sizes, as measured on the electron image plates, correspond to the size of their equivalent sphere from which their unperturbed radius of gyration, R_G, can be calculated. Sizes calculated from our measurements were, within experimental error, in good agreement with sizes obtained by us from light scattering close to Θ conditions,[2] and from literature data on unperturbed R_G's.[5,6]

Our observations led us to propose an explanation[1] to the SANS observations of Ballard et al.[7-10] where the R_G of deuterated polyethylene (PE) molecules dispersed in undeuterated PE did not change measurably upon crystallizing from the melt. Accordingly, because of their higher segmental density, the submolecular domains would be less entangled and interpenetrated by segments belonging to other molecules. Therefore, incipient crystallization will occur within the submolecular higher density domains. Further crystallization may involve additional domains belonging to the primary or other molecules, initially within the volume pervaded by said primary molecule. Such a crystallization process does not necessitate a high level of intermolecular disentanglements and leaves the R_G of the macromolecules unchanged upon going from the melt to the crystalline solid.

For the purpose of verifying this proposed explanation, the following experiments were conceived. Tagged isotactic polystyrene (TiPS) is to be molecularly dispersed in untagged isotactic polystyrene (iPS) to produce some samples in which the TiPS and iPS are semicrystalline. The shape and segmental density of the individual molecules of visible TiPS would be determined. If the submolecular domains tend to crystallize independently, then one expects to find minute crystallites of the TiPS within the confines of its macromolecules. Such crystallites may, conceivably, organize into minute lamellae which may also be observed while still enclosed in the volume pervaded by the parent TiPS molecule. With TiPS being dispersed in iPS, lamellae containing small blocks of TiPS and iPS may form. The lamellae should be best observed when viewed edge on, and a lamella of a given size containing only TiPS should be better defined than those containing both TiPS and iPS because of the former higher electron density.

Conversely, highly crystalline polymer may reveal what happens when whole lamellae traverse through the volume pervaded by individual molecules: does a whole macromolecule "reel in" into the growing lamella, or merely submolecular domains being incorporated into said lamella. To check on this point, tagged ultra-high molecular weight (UHM) polyethylene was to be dispersed in its untagged counterpart. It was hoped that in this fashion one may be able to observe both the tagged macromolecules and the crystalline lamellae traversing through their pervaded volumes.

Experimental Section

Tagged Isotactic Polystyrene. The iPS used in this study, of $M_w = 1.78 \times 10^6$, was obtained from Polysciences, Inc. (cat. No. 2963 and Lot No. 911-3). The tagging was achieved by partial iodination of the iPS in the para position according to the procedure of Braun[11] to a level of 12.83 wt % of iodine. This iodination process was demonstrated by Braun and co-workers[11,12] not to decrease the molecular weight, M, of the polymer and to proceed in a random manner along the polymer chain. The immunity of the PS chain bonds to attack by the reaction mixture should preclude isomerization from isotactic to atactic PS.

0024-9297/79/2212-0265$01.00/0

Table I
Sample Description of TiPS in iPS

code	% TiPS	cast or molded	annealing conditions
19A	5	cast	none
37B	5	cast	6 h/180 °C
19C	5	cast	2 h/150 °C
19D	10	cast	none
37E	10	cast	6 h/180 °C
19F	10	cast	2 h/150 °C
42D	10	molded	none
42D-A	10	molded	2 h/150 °C
48	10	molded, then cast	18 h/165 °C[a]

[a] Opacity due to crystallization was observed after 2 h at the anneal temperature. It did not change noticeably thereafter.

Premeasured amounts of TiPS and iPS were dissolved upon heating under nitrogen atmosphere in redistilled nitrobenzene to yield homogeneous solutions. To prepare solution cast films, the solutions were cast in shallow trays and the solvent was removed at about 50 °C in a forced air draft. The resultant films were further dried under vacuum at about 50 °C to yield films of 0.3 to 0.6 mm thickness. To prepare molded films, the hot nitrobenzene solutions were poured into a large excess of agitated acetone and the polymer collected, washed, dried, and finally molded at about 260 °C for 15 s under a pressure of about a ton per cm^2 film to yield 5-mils thick films. Both kinds of films were annealed when desired under conditions described in Table I.

Percent crystallinity was determined by X-rays, following the standard procedure of Herman and Weidinger,[13] in a Norelco diffractometer with Cu radiation, in parafocus geometry.

The samples were prepared for electron microscopy by microtoming sections of 900 to 1000 Å in thickness, as was described in the previous papers.[2-4] The segmental density distribution within the photographed particles was obtained from microdensitometer scans across their images on the electron image plates, as was described in detail in ref 2 and 3.

Several slices were obtained from each sample and studied in the electron microscope. From the hundreds of grid squares observed, over 100 typical photomicrographs were taken. The photographs presented in this communication are typical. Similarly, the microdensitometer scans presented here are typical of a much larger number of scans obtained from the electron image plates. Unless specified, the procedures above are similar to those employed for the preparation and study of the tagged in untagged PE samples.

Determination of the Number of Tagged Molecules per Visible Tagged Entity. Two procedures were used in order to evaluate whether apparently individual tagged macromolecules are indeed individual molecules or aggregates thereof. Both procedures used the opacity, O, which is the inverse of the transmission, $O = 1/T$, or the related blackening or density D, defined as $D = \log O = \log 1/T$, of the imaged tagged entity to compare with the opacity of the imaged untagged matrix. Assuming that the sample thickness in the neighborhood of such a tagged entity is reasonably uniform, the opacity can be related to the electron density of the imaged entity in the following, related ways: (1) On the electron image plates, the negatives, the opacity is inversely proportional to the electron density of the imaged particle. (2) On the print, the positive, the opacity is directly proportional to the density of the imaged particle.

For the evaluation procedures, images of tagged in untagged iPS were obtained under exactly the same conditions of magnification, beam intensity, exposure, and plate developing. Note that the exposure E is the product of the intensity of the beam impinging on the electron image plate and the duration of the exposure.[14] The printing of the positives, from the negative plates, was performed under as close as possible conditions and variations in these conditions, when existed, tended to minimize the differences between the extremes of intense blackness and intense whiteness of the prints. Such differences usually did not occur on the same prints, and minor changes in the degree of grayness of both the tagged entity and untagged matrix did not affect the results, since the conclusions depend on the ratio of opacity of

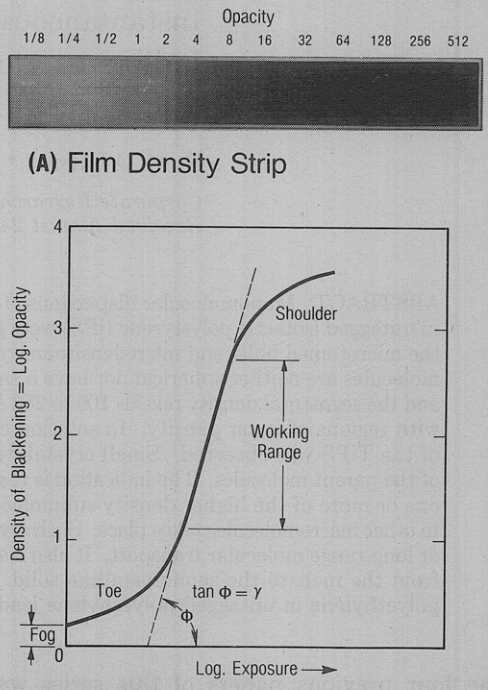

Figure 1. Calibrated film density strip and characteristic curve for density measurements on photomicrographs and electron image plates and their densitometer scans.

the tagged and the untagged material, more than on the corresponding absolute values. The darkness of the entities and backgrounds in the prints were estimated by comparison with a calibrated density strip, shown in Figure 1A, according to procedures commonly used in photography[15,16] and X-ray studies.[14,17] In general, background opacity was in the range of 1 to 4 (D = 0.00 to 0.602) while the opacity of phase separated, intensely black particles was in the range of 125 to 250 (D = 2.097 to 2.398). The opacities of apparently individual tagged macromolecules were usually about twice that of the untagged background; i.e., for a background of opacity 1 the tagged molecule appeared to have an opacity of the order of 2, and for a background opacity of 4 the tagged molecule had an opacity of the order of 8. As will be presently shown, this opacity ratio is close to the ratio calculated for the tagged macromolecules in our particular samples.

The second method of comparison was through a characteristic curve of optical density vs. exposure (time or intensity) of electron image plates. A series of such calibration plates were exposed for given durations in the microscope at a fixed beam intensity and in the absence of a sample. They were then developed under identical conditions. From microdensitometer scans of the exposed and unexposed sections of the plates a characteristic curve of density (log O) against log exposure, in Figure 1B, was constructed, showing the usual[14] toe at very low exposures, the linear working range at higher exposures (up to about $D \simeq 2.5$), and the saturation shoulder at higher exposures. The densitometer scans across electron images of the desired samples, obtained under the same instrumental setting, produced a ratio of opacity between the images of the tagged entities and the image of the untagged background. For apparently individual tagged macromolecules, the ratio of opacity between the tagged entity and the untagged neighboring matrix was routinely in the range of 2 to 2.5. This is in reasonably good accord with the results obtained by the visual comparison of intensities on the prints and, as will be shown, is in agreement with the calculations based on individual tagged molecules in untagged matrix. Because of the very large density difference between the fully phase separated tagged entities and the surrounding untagged matrix, one could not obtain on the same densitometer setting a scan of the untagged matrix together with both a single tagged macromolecule and a tagged phase separated aggregate. Because of the drastically reduced instrumental sensitivity required for the trace of tagged aggregates in untagged matrix, the trace of individual tagged macromolecules

simply blends with the trace of the untagged matrix. In such cases, however, the visual comparison of the electron image plate itself with the calibrated density strip was remarkably effective.

The tagged iPS used in this study contained 12.83% iodine as the tagging species. Conversion to molar ratio yielded a composition of 61.63 CH units per each I atom. The opacity of a given submolecular volume element, $d\upsilon$, is proportional to the sum of the scattering atoms in said $d\upsilon$ times the square of the number of electrons each such atom has.[17] The ratio of the opacities of the tagged and untagged substances is the number we are interested in.

For the iodine-tagged iPS the opacity, O_{TiPS}, is, then,

$$O_{TiPS} \propto \Sigma(f_C)^2 + \Sigma(f_H)^2 + \Sigma(f_I)^2$$

$$O_{TiPS} \propto 61.63(6)^2 + 61.63(1)^2 + 1(53)^2 = 5089.31$$

and for the untagged iPS the opacity, O_{iPS}, is

$$O_{iPS} \propto \Sigma(f_C)^2 + \Sigma(f_H)^2$$

$$O_{iPS} \propto 61.63(6)^2 + 61.63(1)^2 = 2280.31$$

The ratio of the opacities will, then, be

$$\frac{O_{TiPS}}{O_{iPS}} = \frac{5089.31}{2280.31} = 2.232$$

and log 2.232 is $D_r = 0.3487$ with D_r being the relative density. This indicates that a volume element $d\upsilon$ of iodized iPS will be more opaque by 2.232 than the corresponding volume element of untagged iPS. If a tagged macromolecule will collapse upon itself, or if more than one tagged molecule will share the same pervaded volume, then the concentration of tagging species (iodine in our case) in each $d\upsilon$ within said volume will be higher than calculated and the opacity of the image of the $d\upsilon$ volume element will be higher too. If, for instance, two tagged macromolecules share the same pervaded volume then the opacity of each $d\upsilon$ within said volume will be

$$O_{TiPS} \propto 61.63(6)^2 + 61.63(1)^2 + 2(53)^2 = 7898.31$$

and its ratio to the opacity of the untagged polymer will be

$$\frac{O_{TiPS}}{O_{iPS}} = \frac{7898.31}{2280.31} = 3.464$$

leading to $D_r = 0.5396$.

As was previously stated, the actually observed opacities of the apparently individual tagged macromolecules were about 2 to 2.5 times larger than the opacities of the corresponding untagged backgrounds. Therefore, one may conclude that the individual tagged macromolecules are not apparently individual, but individual indeed.

Macromolecules of $M > 1 \times 10^6$, of the size employed in this study, constitute no more than 1% of their pervaded volume in the unperturbed state.[18] In the bulk, the other ≥99% are taken up by segments belonging to other molecules. If a tagged molecule collapses to comprise 100% of its pervaded volume, or if a phase separation segregated the tagged molecules in aggregates, then the density of each submolecular $d\upsilon$ will reflect the very large increase in the concentration of the tagging species. On the other hand, the opacity due to the scattering by carbon and hydrogen atoms will remain about the same (except for density effects), since it is immaterial whether the CH species originate from the tagged or untagged molecules. For an increase from 1 to 100% concentration of tagged molecule, the opacity will accordingly increase to

$$O_{TiPS} \propto 61.63(6)^2 + 61.63(1)^2 + 100(53)^2 = 283180.31$$

and

$$\frac{O_{TiPS}}{O_{iPS}} = \frac{283180.31}{2280.31} = 124.185$$

leading to log 124.185 = $D_r = 2.094$. This value is in the range of intensely black images on the printed positives, in agreement with our results and the calibrated density strip used in the visual estimates of the opacity.

It is our strong belief, then, that entities observed as individual TiPS macromolecules are indeed individual molecules. In the following Results section, they will be so referred to.

The sizes of the observed entities were measured on calibrated electron micrographs. The results were compared with unperturbed molecular sizes calculated according to the formula

$$D = 2R_G(5/3)^{1/2}$$

where D is the unperturbed diameter of the equivalent sphere. Because of the low iodine tagging, it was assumed that the R_G of TiPS is the same as for an iPS molecule of the same length. From data in ref 5 and 6, the R_G of the TiPS used in this work was calculated to be 365 Å and its D = 950 Å.

Tagged Ultra-High Molecular Weight Polyethylene. For the purpose of determining whether one can observe with the electron microscope instances where lamellae traverse the pervaded volume of tagged molecules without these volumes collapsing into the lamellae, observations on ultra-high molecular weight polyethylene (PE) were carried out. Two molecular weights were used: one was $M_v = 2.8 \times 10^6$ (Allied Chemical Corp. AC 1220, of rather broad molecular weight distribution), and the other was of viscosity average molecular weight, M_v, of 10×10^6 (Allied Chemical Corp. experimental PE 260-100). The tagging procedure was conducted as follows: By heating with stirring at about 135 °C, a dilute solution (<0.5%) of each polymer in tetrachloroethane (TCE) containing some antioxydant was prepared. Once the polymer dissolved, the temperature was reduced to about 120 °C, making sure that no precipitation or gelation takes place. Elemental bromine, in excess of the amount to be consumed, was added through a pressure equalizing funnel. (**Caution**! Run the reaction vented in a proper hood and behind a safety shield.) After a uniform mixing of the solution was attained, a high-intensity UV lamp was turned on, illuminating the glass reaction vessel for the desired duration. Depending on the desired level of bromination, the reaction took anywhere from 2 to 30 min, with polymer degradation becoming more pronounced the longer the reaction took. Higher temperatures were also conducive to polymer degradation. After carefully washing the polymer, a cycle of redissolving in hot xylene or decalin, followed by precipitation in methanol or acetone, was twice repeated. Finally, the polymer was dried under vacuum and its bromine content determined by elemental analysis. The M_v of the brominated polymer was calculated from its intrinsic viscosity in decalin, assuming that the brominated polymer follows the same M_v–viscosity relation as untagged PE. From many such runs, the following bromine-tagged polyethylenes were selected to be used: (1) originating from PE of $M_v = 2.8 \times 10^6$, a 23.7 wt % of brominated PE having a $M_v = 2.9 \times 10^6$ (intrinsic viscosity = 14.9 dL/g); and (2) originating from PE of $M_v = 10 \times 10^6$, a 6.42 wt % of brominated PE having a $M_v = 8.1 \times 10^6$ (intrinsic viscosity = 28.8 dL/g).

The Br-tagged polymer was dissolved with a ninefold amount of its untagged counterpart in decalin, and after a complete dissolution and thorough mixing, the solution precipitated into agitated methanol. The solid polymer was filtered and, after careful drying, the mixture containing 10% tagged PE was molded in a press under one ton per cm² film for 1 min at 190 °C to form films 3 mils thick. The films were then quick quenched (within a second or two) in ice water. Similar films were prepared from the untagged and from the tagged corresponding polymers. Some of the films were annealed for 2 h at 70 ± 5 °C, but when the percent crystallinity was measured, it was found that all the molded PE films, quick quenched or annealed, had 40–60% crystallinity with no significant difference between each pair of annealed and unannealed material of the same composition. Moreover, the diffraction patterns of the untagged, tagged, and mixed PE samples were all the same within experimental error. The similarities in percent crystallinity and diffraction patterns indicate that at the level of bromination used in our experiments, the polymer still maintains the crystal characteristics of the untagged PE.

The polyethylene films used for electron microscopy were microtomed at liquid nitrogen temperatures, as described in ref 2 and 3, to yield slices about 1000 Å in thickness. These were mounted on grids and observed in the transmission mode without shadowing. The percent crystallinity of the tagged, $M_v = 8.1 \times 10^6$, dispersed in untagged, $M_v = 10 \times 10^6$, PE was 58 ± 2% and that of the tagged, $M_v = 2.9 \times 10^6$, dispersed in $M_v = 2.8 \times 10^6$ PE was 48 ± 2%. The percent crystallinities of the corresponding

untagged polymer films, used as blanks for comparison, were the same as those of the mixed samples.

From data in ref 5 and 6, the R_G of PE of $M_v = 8.1 \times 10^6$ was calculated to be 1220 Å and the diameter of the equivalent sphere 3150 Å. The R_G of the untagged PE of $M_v = 2.8 \times 10^6$ was calculated to be 720 Å and its diameter of equivalent sphere 1850 Å. Throughout this work it was assumed that the dimensions of the tagged PE are a close approximation of the untagged PE of similar chain length. It was thus taken that the R_G of an untagged PE of $M_v = 8.1 \times 10^6$ will correspond to the R_G of the tagged PE of the same length, and that the R_G of the untagged PE of $M_v = 2.8 \times 10^6$ will correspond to that of the tagged PE of $M_v = 2.9 \times 10^6$.

Results

Tagged Isotactic Polystyrene. Visual observations of the photomicrographs of samples showing no phase separation reveal that, in accord with the previous observations,[1-4] the instantaneous shape of individual TiPS macromolecules, in the amorphous state, is not exactly spherical and possesses a somewhat irregular perimeter. The microdensitometer scans revealed high-density regions within the confines of each macromolecule, the size of which is 100 to 250 Å. As was noted previously for both PIP and PS, these higher density domains are held together by lower density material, and tend to aggregate closer to the center of the macromolecule.[1-4] The size of the macromolecules, as measured on the calibrated electron micrographs and on the densitometer scans, ranges from about 600 to 1100 Å with a preponderance at 750 to 900 Å, reasonably close to their calculated unperturbed size of 950 Å.

The percent crystallinity in TiPS in iPS cast films was found to hover at about 16% and to be independent of the thermal history of the film. For example, samples 19A, 19C, and 37B were all within the narrow interval of 16.46 ± 0.3% crystallinity. The molded samples 42D and 42D-A, on the other hand, showed no crystallinity measurable by X-ray techniques. However, when an amorphous molded TiPS in iPS sample was redissolved in nitrobenzene and cast into a new film, sample 48, 14% crystallinity was measured.

The molded films showed no crystallinity by X-rays. By electron microscopy, the unannealed samples showed an extremely small amount of crystallinity. This crystallinity, in the form of microcrystallites, was visible in the electron micrographs as minute specks and streaks. After annealing, a significant increase in crystallinity visible by electron microscopy appeared in the regions of TiPS in iPS that did not undergo a pronounced phase separation during the annealing process. This crystallinity, however, was still below the about 1% necessary for detection by X-ray techniques.

The experiments above indicate that the iPS of $M = 1.78 \times 10^6$ used in this study, and the TiPS prepared from it, show a strong reluctance to change their percent crystallinity by heat treatment alone and require the presence of some solvent to act as a plasticizer and facilitate some crystallization.

In general, the unannealed molded samples showed more phase separation than the solution cast ones. Figure 2, of the molded unannealed TiPS in iPS, sample 42D, shows a moderate amount of phase separation. At the same time, there are hardly any TiPS crystallites visible in the sample. Two hours of annealing at 150 °C, in sample 42D-A in Figure 3, caused no measurable change in the level of phase separation. On the other hand, a considerable number of dense crystallites, on the order of 200 to 400 Å in size, become visible. Areas of the same sample, usually closer to the surfaces of the bulk film, which were more phase separated, are characterized by Figure 4. A considerable amount of crystallites can be seen in the right-hand side of the photograph, in areas not swept clean of TiPS in the process of phase separation.

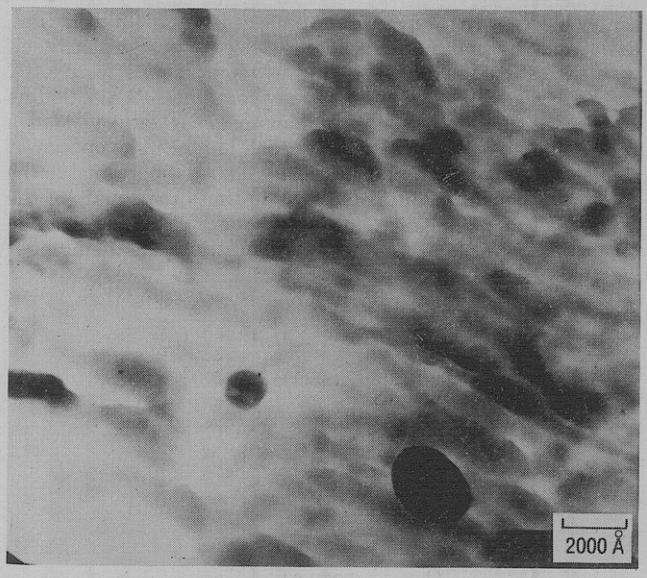

Figure 2. Typical area of unannealed molded TiPS in iPS.

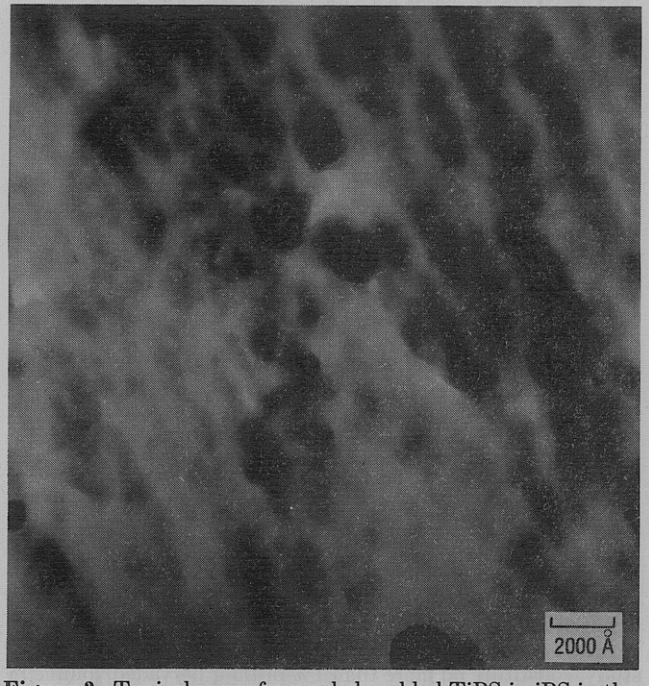

Figure 3. Typical area of annealed molded TiPS in iPS in the absence of significant phase separation.

In contrast to the scarcity of crystallites in the molded samples, annealed or not, samples originating from solution casting show a multitude of crystallites. This goes hand-in-hand with the large increase in percent crystallinity, from less than 1% (the threshold of detection by X-rays) in the molded films to about 16% in the cast ones. Figure 5 is typical of the unannealed sample 19A and Figure 6 is characteristic of the annealed sample 19C. A comparison of Figures 2 and 5 reveals that in the latter many more crystallites of 200 to 400 Å are visible. Their number in Figure 6 is considerably larger than in Figures 5 and 3. It is obvious that upon annealing of solution cast films, a large increase in the number of crystallites, visible as dark streaks and specks in the photomicrographs, becomes apparent. In general, it appears that the shape and the crystallization pattern of the TiPS molecules are

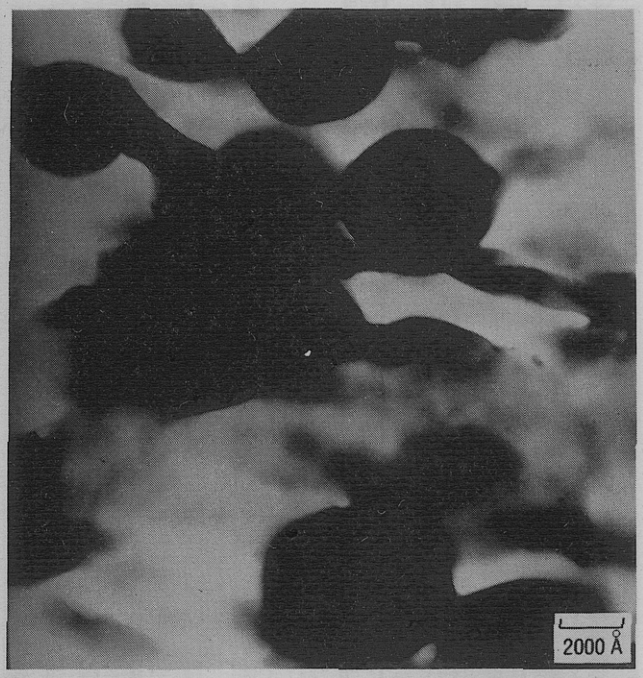

Figure 4. Areas of annealed molded TiPS in iPS where significant phase separation took place.

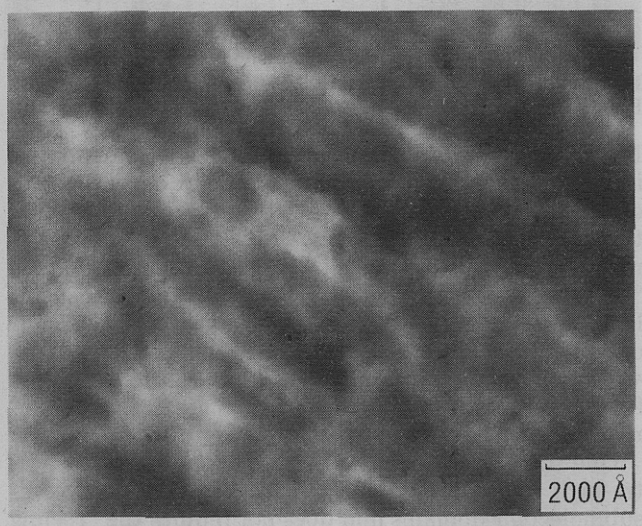

Figure 5. Characteristic area of unannealed cast TiPS in iPS.

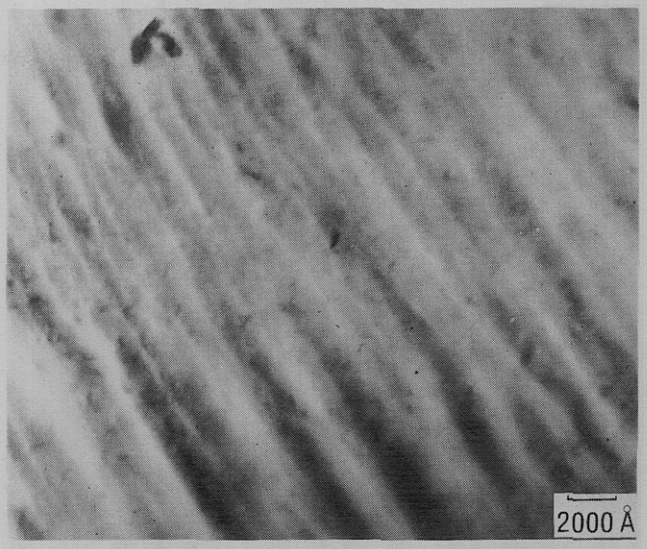

Figure 6. Characteristic area of annealed cast TiPS in iPS.

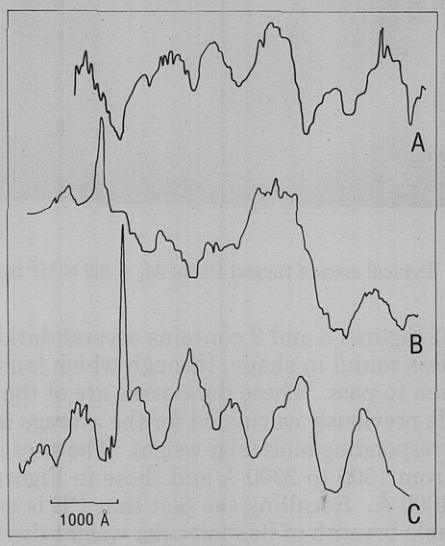

Figure 7. Traces of microdensitometer scans across unannealed (trace A) and annealed (traces B and C) TiPS in iPS. The spikes on the left-hand side of traces B and C correspond to traversals across the thickness of lamellae observed edge on in the electron image plates.

not observably affected by the concentration of TiPS in the sample.

Recall that in the transmission mode in the electron microscope, the TiPS-containing lamellae and crystallites are observed best when viewed edge on. As can be seen, say, in Figure 6, the edge-on lamellae are about 150 Å in thickness and 200 to 400 Å in length. This thickness is in accord with the total thickness (crystalline plus amorphous) obtained for iPS lamellae by SAXS and reported recently by Stein et al.[19] It appears that the edge-on lamellae observed by us include a substantial amount of amorphous (unmeasurable by X-ray crystallinity detection techniques) material adhering to the lamellar fold surfaces.

The minute lamellae are almost always present within the confines inscribed by individual macromolecules. This becomes especially clear when we study the microdensitometer scans presented in Figure 7. Here, the upper curve A is typical of the TiPS macromolecules suspended in iPS in the amorphous unannealed state. Curves B and C are scans across areas each containing a lamella visible edge on. The sharp spikes in the scans reflect the high density of the image of the edge-on observed lamellae. In hardly any case a halo of electron-dilute matter is to be seen around individual minute lamellae. We believe this indicates that nascent crystallization, forming these minute lamellae, takes place within individual submolecular domains of high segmental density and does not involve the (very large) molecule as a whole.

Tagged Ultra-High Molecular Weight Polyethylene. Figures 8 and 9 are of 10% tagged PE of $M_v = 2.9 \times 10^6$ and $M_v = 8.1 \times 10^6$ in untagged PE of comparable molecular weight, correspondingly. The dark area in the upper left-hand side of Figure 8 arose from the electron beam passing through several layers of sample caused by folding over of the microtomed slice. While the untagged blanks yielded, under identical conditions, very poorly resolved lamellar structures and extremely poor contrast, the mixtures in Figures 8 and 9 exhibited a surprisingly high level of lamellar resolution and high contrast. In light of the fact that the polymer mixtures in Figures 8 and 9 have about the same percent crystallinity and the same X-ray diffraction patterns as those of the untagged blanks, the reason for the high contrast and resolution is not clear to us.

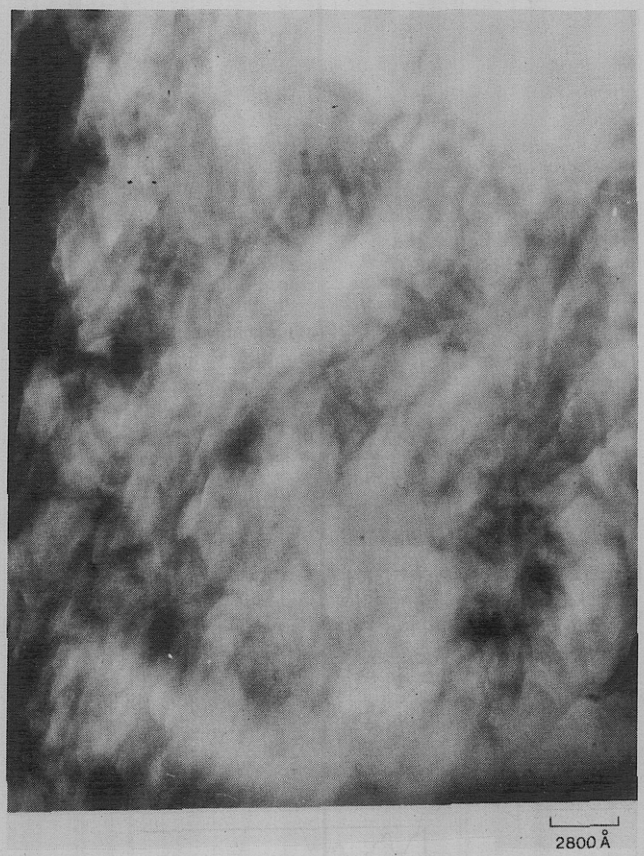

Figure 8. Typical area of tagged PE of $M_v = 2.9 \times 10^6$ in untagged PE.

Figure 9. Typical area of tagged PE of $M_v = 8.1 \times 10^6$ in untagged PE.

Each of Figures 8 and 9 contains several darker areas, more or less round in shape, through which lamellae are clearly seen to pass. These dark areas are of the order of magnitude previously calculated for the average molecules of the corresponding molecular weight. The sizes in Figure 8 range from 1500 to 2000 Å and those in Figure 9 from 2500 to 4000 Å. Recalling the fact that PE is usually of considerable breadth of its molecular weight distribution, the observed sizes are gratifyingly close to the expected ones. We may, thus, tentatively conclude that the darker entities in Figures 8 and 9 are indeed tagged PE molecules, and that lamellae can pass through the volumes pervaded by such molecules without these molecules collapsing upon themselves or being fully incorporated into the growing lamellae.

If, conversely, the dark areas in Figures 8 and 9 are considered not to be associated with individual tagged macromolecules, then the latter must be assumed uniformly distributed throughout the samples since no evidence of segregation of the tagged PE out of the untagged PE was observed by us. Since we observe no regions within given lamellae substantially darker (more dense) than adjacent regions in the very same lamellae, one cannot assume that whole tagged macromolecules crystallized upon themselves, by the conceivable process of "reeling in", into whole lamellae or individual sublamellar dense crystalline blocks.

Accepting, or not accepting, that the dark regions in Figures 8 and 9 are images of individual tagged PE molecules leads to the very same conclusion: large PE lamellae can traverse through distances corresponding to the pervaded volumes of the macromolecules. These lamellae contain submolecular parts of the macromolecules, with the tagged and untagged polymer co-crystallizing in the same lamella without recourse to a "reeling in" of whole molecules. In the ultra-high molecular weight PE material used in this study, the "reeling in" process is practically excluded, since the quick quenching procedure took a second or two while the maximum relaxation times τ_m, required for motions of whole molecules, are much longer. It was shown by Aloisio et al.[20] that at 200 °C the τ_m of PE of $M_w = 79\,000$ is about 1 s. Since τ_m is linearly related to the molecular weight,[21,22] the τ_m for PE of $M_v = 2.8 \times 10^6$ at 190 °C must be 35 s and that of $M_v = 8.1 \times 10^6$ much longer. As the temperature is lowered from the molding temperature, τ_m increases more and more.

One thus may conclude that the crystallization of ultra-high molecular weight PE from the melt involves submolecular domains and does not require the "reeling in" of whole macromolecules. The R_G of the macromolecule remains, therefore, the same in the melt and in the crystallized bulk, in agreement with neutron scattering observations.[7-10]

References and Notes

(1) S. M. Aharoni, *Polym. Prepr., Am. Chem. Soc., Div. Polym. Chem.*, **19** (1), 461 (1978).
(2) S. M. Aharoni, *Polymer*, **19**, 401 (1978).
(3) S. M. Aharoni, *J. Macromol. Sci., Phys.*, **15**, 635 (1978).
(4) S. M. Aharoni, *Macromolecules* **11**, 677 (1978).
(5) M. Kurata and W. H. Stockmayer, *Fortschr. Hochpolym.-Forsch.*, **3**, 196 (1963).
(6) M. Kurata, Y. Tsunashima, M. Iwama, and K. Kamada in "Polymer Handbook", 2nd ed., J. Brandrup and E. H. Immergut, Eds., Wiley-Interscience, New York, 1975, p IV-1 ff.
(7) J. Schelten, G. D. Wignall, and D. G. H. Ballard, *Polymer*, **15**, 682 (1974).
(8) J. Schelten, D. G. H. Ballard, G. D. Wignall, G. Longman, and W. Schmatz, *Polymer*, **17**, 751 (1976).
(9) D. G. H. Ballard, J. Schelten, and A. Cunningham, *Polymer*, **18**, 259 (1977).
(10) D. G. H. Ballard, J. Schelten, and G. W. Longman, *Polym. Prepr., Am. Chem. Soc., Div. Polym. Chem.*, **18** (2), 167 (1977).
(11) D. Braun, *Makromol. Chem.*, **30**, 85 (1959).
(12) D. Braun, D. Chaudhari, and W. Machtle, *Angew. Makromol. Chem.*, **15**, 83 (1971).

(13) P. H. Hermans and A. Weidinger, *J. Appl. Phys.*, **19**, 491 (1948).
(14) H. P. Klug and L. E. Alexander, "X-ray Diffraction Procedures", Wiley-Interscience, New York, 1974, pp 114–116.
(15) H. P. Rockwell, Jr., in "The Encyclopedia of Photography" Vol. 5, National Educational Alliance, N.Y., 1949, pp 1609 and 1610.
(16) J. N. Harman, Jr., in "The Encyclopedia of Photography", Vol. 5, National Educational Alliance, N.Y., 1949, p 1899 ff.
(17) G. H. Stout and E. H. Jensen, "X-ray Structure Determination", Macmillan, London, 1968, pp 165–177 and 200–211.
(18) C. Tanford, "Physical Chemistry of Macromolecules", Wiley, New York, 1961, p 178.
(19) F. P. Warner, W. J. MacKnight, and R. S. Stein, *J. Polym. Sci., Polym. Phys. Ed.*, **15**, 2113 (1977).
(20) C. J. Aloisio, S. Matsuoka, and B. Maxwell, *J. Polym. Sci., Part A-2*, **4**, 113 (1966).
(21) W. W. Graessley, *Polym. Prepr., Am. Chem. Soc., Div. Polym. Chem.*, **13** (1), 35 (1972).
(22) S. M. Aharoni, *J. Macromol. Sci., Phys.*, **13**, 159 (1977).

Rigid Backbone Polymers. 4. Solution Properties of Two Lyotropic Mesomorphic Poly(isocyanates)

Shaul M. Aharoni* and Eugene K. Walsh

Corporate Research Center, Allied Chemical Corporation, Morristown, New Jersey 07960.
Received October 24, 1978

ABSTRACT: Solution properties of poly(hexyl isocyanate) (PHIC) and poly(50% butyl + 50% *p*-anisole-3-propyl isocyanate) (PBAPIC) polymers were evaluated by M_w, M_n, viscosity, and microscopic techniques. The results show: (a) both polymers form liquid crystals above a certain critical concentration; and (b) both polymers partition into more concentrated anisotropic and more dilute isotropic phases (the anisotropic phase is composed of the higher molecular weight fraction of the polymer and the isotropic phase contains the lower molecular weight portions of the polymer). Microscopic observations of isotropic inclusions in the anisotropic solution phase of PHIC reveal the former to possess angular shapes. The development of this angularity is explained as resulting from the growth of the isotropic inclusions.

A statistical thermodynamic theory applicable to concentrated solutions of polydisperse rigid polymers was recently put forth by Professor Flory.[1] Accordingly, in the event that a concentrated solution of rigid polymer molecules separates into a disordered, isotropic phase and an ordered, anisotropic phase, the higher molecular weight, M, fractions would preferentially partition into the anisotropic phase, and the lower M fractions would concentrate in the isotropic phase. Furthermore, the theory shows that the concentration, c, of the polymer in the anisotropic phase will be substantially higher[2] than in the isotropic phase.

We have recently discovered[3,4] that many poly(isocyanate) polymers exhibit lyotropic and thermotropic mesomorphic behavior. The poly(isocyanates) capable of forming liquid crystals may be divided into the following three categories: (a) poly(alkyl isocyanate) homopolymers having side chains $4 \leq n \leq 12$ long, n being the number of carbon atoms in the normal alkyl side chain; (b) poly(alkyl–aralkyl isocyanate) copolymers in which the aromatic residue is at least two $-CH_2-$ groups removed from the chain backbone; and (c) substituted homo- and copolymers, and certain poly(alkyl isocyanate) copolymers.

Because of the relative simplicity of their preparation, and especially because of the high solubility of many members of the poly(isocyanate) family in common solvents, these polymers lend themselves to studies of liquid crystal polymers in general and to tests of the theory expounded in ref 1 in particular.

In this paper we wish to report results of studies conducted on two polymers: poly(hexyl isocyanate) (PHIC), and poly(50% butyl + 50% *p*-anisole-3-propyl isocyanate) (PBAPIC). (The monomer composition of the copolymer was determined by nuclear magnetic resonance (NMR) spectroscopy and is given in mol %.)

Experimental Section

The polymers were prepared according to the general procedure of Shashoua[5,6] as described in detail in ref 3. Butyl and hexyl isocyanate were obtained from Aldrich Chemicals and Eastman Chemicals, respectively, and were used without further purification. The comonomer *p*-anisole-3-propyl isocyanate was prepared[3] from 4-(*p*-methoxyphenyl)butyric acid which was procured from Aldrich Chemical Co.

Dilute solution viscosities were determined in Cannon–Ubbelohde glass viscometers operating at low to medium shear rates in a constant temperature bath set at 25 °C. The solvents most often used were 1,1,2,2-tetrachloroethane (TCE), chloroform, bromoform, and toluene. Concentrated solution viscosity was determined with the aid of a Nametre Direct Readout Viscometer operating at a fixed shear rate of 4060 s^{-1}, at 25 °C. The polymer batches studied with the Nametre Viscometer were of such a low molecular weight (M_w of PHIC was 65 000 and of PBAPIC about 35 000) that they did not show a significant increase in the viscosity when measured in several rapid consecutive runs. The same behavior was observed in the dilute solution glass viscometers for the low-M batches. High-M batches showed substantial increases in viscosity in several rapid runs on the same solution. When the solution relaxes overnight, the measured viscosity was, within experimental error, the same as the initial viscosity.

Light-scattering measurements were performed at 5461 Å wavelength on solutions maintained at ambient temperature in a Brice–Phoenix spectrophotometer. Weight average molecular weights, M_w, were obtained from dilute $CHCl_3$ solutions of polymer fractions isolated from the anisotropic and isotropic solution phases by the Zimm plot[7,8] method. Number average molecular weight, M_n, was determined in a Mechrolab membrane osmometer using chloroform and chlorobenzene solvents. Polarized light microscopy was performed in a Leitz Ortholux polarized light microscope. Because it is an excellent solvent for most poly(isocyanates) and evaporates relatively slowly at room temperature, TCE was the solvent of choice for most of the optical microscopy work. It should be noted, however, that mesogenic polymers were mesomorphic in quite a few solvents, once the critical concentration for the formation of the anisotropic phase, v_2^*, was surpassed.

Compositional studies were performed by means of a Varian A-60 NMR instrument on solutions of the polymers in deuterated TCE. The density of the polymers was determined by pycnometry in aqueous solutions of $ZnCl_2$, or in mixtures thereof with small amounts of methanol.

Results

When concentrated solutions of PHIC in solvents such as TCE, chloroform, bromoform, and toluene or PBAPIC

0024-9297/79/2212-0271$01.00/0